Adsorption of cationic and anionic dyes by ethylenediamine-modified carboxymethyl cellulose

Wenjuan Chen, Yunshan Bai*, Min Wu, Hongzhu Ma*

School of Chemistry and Chemical Engineering, Shaanxi Normal University, Xi'An, Shaanxi 710119, China, Tel. +86 29 81530726; Fax: +86 29 81530727; email: hzmachem@snnu.edu.cn (H. Ma)

ABSTRACT

A novel amphoteric adsorbent, ethylenediamine-modified carboxymethyl cellulose (EDA-CMC$_x$) with various CMC amounts, was prepared to eliminate toxic methylene blue (MB) and orange II (ORII) dyes from wastewater. The modification and adsorption onto EDA-CMC$_1$ was analyzed by Fourier transform infrared spectroscopy, scanning electron microscopy, energy dispersive spectroscopy, thermogravimetric analysis, and zeta potentials. At 293 K, the maximum adsorption capacities of 82.06 and 63.72 mg g^{-1} for 250 mg L^{-1} MB and ORII, respectively, were obtained at pH 11 (MB) and pH 3 (ORII) within 30 min. Various zeta potentials were obtained (+10 mV at pH 3 and −30 mV at pH 11) and pH-sensitive properties of EDA-CMC$_1$ were exhibited during the adsorption process. The adsorption of ORII followed the Langmuir isotherm, while MB adsorption could be described better by Freundlich model. For adsorption kinetics, both of them followed the pseudo-second-order kinetics equation. These results indicated that EDA-CMC$_1$ could serve as a potential material for textile wastewater treatment.

Keywords: Carboxymethyl cellulose; Ethylenediamine; Adsorption; Methylene blue; Orange II

1. Introduction

Nowadays, the rapid development of industry improves the quality of our life and results in serious environment pollution [1]. The water pollution can negatively affect the aquatic biota and human health even at relative low concentrations. Printing and dyeing effluents was one of the industrial pollutant headstreams. The discharge of effluents that contain synthetic dyes is a major concern to the environment and aquatic life, due to the hazards associated with toxicity and their xenobiotic properties [2,3]. Large quantities of dye effluents are produced by textile dyeing and the dye manufacturing industries. There are more than 10,000 types of dyes in commercial circulation and 2% of dyes produced annually are discharged into water resources during industrial processing, that cause adverse effects on aquatic organisms and human health and urgent to govern before discharge [4,5].

Currently, various technologies, such as adsorption [6,7], membrane separation, flocculation precipitation [8,9], oxidation, catalytic degradation [10], and biodegradation [11] are employed in wastewater management, particularly in dye removal. Among these, adsorption has been studied extensively and applied widely in advanced treatment of the low concentration wastewater because of its low cost, widely material resource, simplicity of design and operation [12,13]. However, the use of adsorption materials with excellent adsorption ability toward dyes is relatively scarce, especially in the study of the adsorption mechanism. Therefore, the search for efficient sorbents and the evaluation of the adsorption mechanism are still going on.

Carboxymethyl cellulose (CMC), with abundant hydroxyl and carboxyl groups, is a derivative of natural cellulose polysaccharide obtained from the carboxymethylation of natural cellulose by reacting with alkali and chloroacetic acid

* Corresponding author.

and widely applied in food, cosmetics, pharmaceutics, and drug delivery system industries due to its low toxicity, low immunogenicity, and biodegradability [14,15]. As an anionic polyelectrolyte material, with sensitive to pH, temperature, and ionic strength, etc., CMC has been effectively used to remove cationic dyes from aqueous solutions through the electrostatic interactions between the negatively charged carboxylate ions and positively charged cationic dyes [16]. However, its application as an adsorbent for dyes removal is limited because of its hydrophilicity and low removal efficiency toward anionic dyes, which can usually be overcame by modifying with cationic compounds. Among various functional groups, the amine group exhibits a relatively high reactivity and can react easily with many chemicals. Salama et al. [5] and Li et al. [17] investigated the cationicmonomer-2-(dimethylamino) ethyl methacrylate (DMAEMA) grafting CMC with excellent adsorption performance toward anionic dyes. Hence it is feasible to introduce N-containing functional group on CMC surface to enhance its adsorption capacity and develop low-cost high efficient absorbents [18]. Ethylenediamine (EDA) is a widely used building block in various chemical synthesis. Therefore, CMC was modified by the cation modifier EDA, and a novel amphoteric adsorbent was prepared and its adsorption properties toward anionic and cationic dyes was investigated.

In this work, ethylenediamine-modified CMC adsorbents with amphoteric adsorption property were prepared. The synthesized adsorbents were characterized by Fourier transform infrared (FT-IR) spectroscopy, scanning electron microscopy (SEM), energy dispersive spectroscopy (EDS), thermogravimetric analysis (TGA), and zeta potentials. Batch adsorption studies were carried out to identify the optimum adsorption conditions such as contact time, pH, initial dye concentration, adsorbent dose, and regeneration of adsorbent. Generally, methylene blue (MB) and orange II (ORII) are presented in wastewater, and here selected as a cationic and an anionic dye model, respectively. Meanwhile, the kinetic and adsorption isotherm models were investigated to better evaluate its adsorption property and behavior. In addition, the possible adsorption mechanism was also proposed.

2. Materials and method

2.1. Materials

Sodium carboxymethyl cellulose (CMC, 300–800 mPa·s, C.P), sodium hydroxide (NaOH, A.R.), epichlorohydrin (ECH, C_3H_5ClO, A.R.), ethanol (C_2H_5OH, A.R.), ethylenediamine (EDA, $H_2NCH_2CH_2NH_2$, A.R.), acetone (CH_3COCH_3, A.R.), methylene blue (MB, $C_{16}H_{18}ClN_3S·3H_2O$, A.R.), orange II (ORII, $C_{16}H_{11}N_2O_4SNa$, A.R.), Congo red (CR, $C_{32}H_{22}N_6NaO_6S_2$, A.R.), methyl orange (MO, $C_{14}H_{14}N_3NaO_3S$, A.R.), malachite green (MG, $C_{23}H_{25}ClN_2$, A.R.), hydrochloric acid (HCl, A.R.), were obtained from Sinopharm Chemical Reagent Co., Ltd., Shanghai, China, and used directly without further purification.

The chemical structures of dyes are summarized in Table 1.

2.2. Preparation of adsorbent EDA-CMC$_x$

The ethylenediamine (EDA)-modified CMC adsorbent was prepared according to the reference reported [19,20].

Typically, into 100 mL 5 wt% NaOH solution containing 1 g CMC, 30 mL of ethanol and 30 mL of epichlorohydrin were added with stirring at 50°C for 4 h. Then 5 mL of EDA was added and the mixture was continuously stirred at 60°C for 2 h. Afterwards, the modified products were precipitated by acetone, filtrated, washed by ethanol and distilled water successively several times, and dried in a vacuum oven at 60°C for 12 h, coded as EDA-CMC$_1$. The synthetic procedure can be illustrated in Fig. 1.

The series of samples treated with 0.5, 1, 1.5, 2, and 3 g of CMC, which were coded as EDA-CMC$_{0.5}$, EDA-CMC$_1$, EDA-CMC$_{1.5}$, EDA-CMC$_2$, and EDA-CMC$_3$, respectively.

2.3. Adsorption experiments

The adsorption experiment of cationic dye (MB) and anionic dye (ORII) were carried out in batches. 30 mg of EDA-CMC$_x$ adsorbent was immersed into 10 mL of the dye solution with different initial concentration of 50, 100, 150, 200, and 250 mg L^{-1} at room temperature (RT: 20°C). The pH of the solutions was adjusted by using 0.05 M HCl or 0.2 M NaOH to the final pH values ranging from 3 to 11, with an agitation speed of 300 rpm. After a certain time, separated the adsorbent, the concentration of dye was then determined by measuring the absorbance of the solution at λ_{max} (484 nm for ORII; 665 nm for MB), using a UV-vis spectrophotometer (UVT6, Beijing Purkinje General Instrument Co. Ltd, China). Before the measurement, a calibration curve of MB or ORII with known concentrations was obtained. The removal (R%) and the adsorption amount (q_t) of ORII and MB can be calculated according to Eqs. (1) and (2) as follows:

$$R\% = \frac{C_0 - C_t}{C_0} \times 100 \tag{1}$$

$$q_t = \frac{(C_0 - C_t)V}{W} \tag{2}$$

where C_0 and C_t (mg L^{-1}) are the concentrations of ORII or MB in solutions at initial time and time t (min), respectively, W (mg) and V (mL) are the amount of adsorbent used and the volume of the dyes solution, respectively.
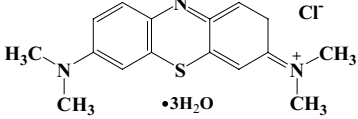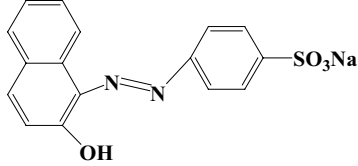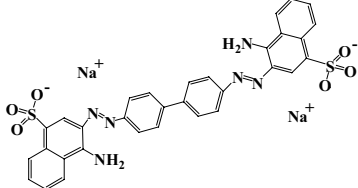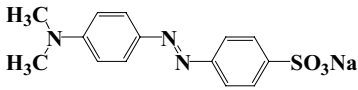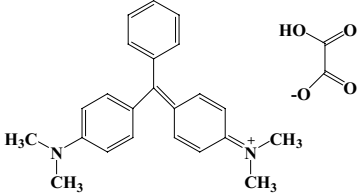
2.4. Regeneration and recycle of EDA-CMC$_1$

For regeneration study, EDA-CMC$_1$ adsorbed ORII or MB was immersed into ethanol solution at pH 3 or 11 with stirring at 300 rpm at RT. After 30 min, EDA-CMC$_1$ was separated and dried in a vacuum oven at 60°C for 12 h. 30 mg regenerated EDA-CMC$_1$ was added in 10 mL 50 mg L^{-1} ORII or MB solution at RT at pH 3 (ORII) or 11 (MB). The sorption–desorption cycles were repeated for five times, and the dyes removal was calculated using Eq. (1).

2.5. Characterization of adsorbents

FT-IR spectra of CMC, EDA-CMC$_1$ before and after adsorption were obtained on FT-IR spectroscopy (Tensor 27,

Table 1
Characteristics of various dyes

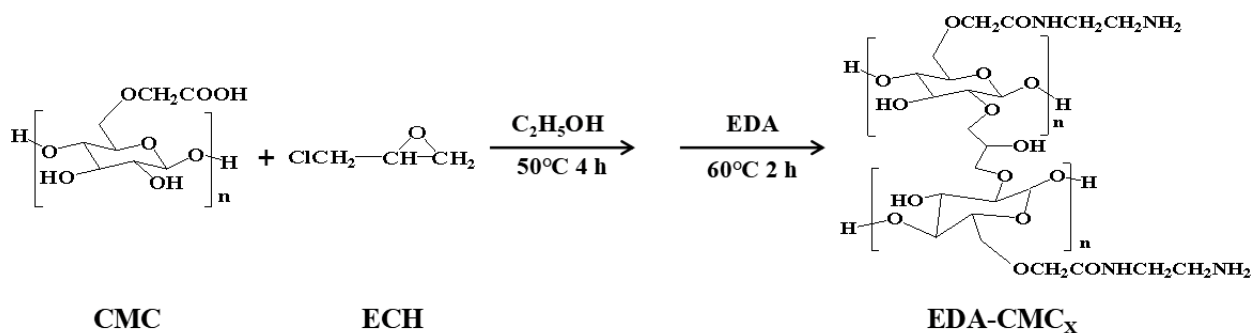| Dye	Molecular structure	Maximum absorption wavelength (nm)
MB (methylene blue)		668
ORII (orange II)		484
CR (Congo red)		497
MO (methyl orange)		507
MG (malachite green)		617

Fig. 1. Synthesis of EDA-CMC$_x$ composites adsorbent.

Bruker, Germany) in the range of 400–4,000 cm^{-1}. The surface morphological measurement of samples was analyzed using SEM (Quanta 200, FEI). Thermal stability was determined using thermoanalyzer systems (TGA, Q600SDT, USA) in the range of 20°C–500°C at a heating rate of 10°C min^{-1}. The zeta potentials of the samples were determined using laser particle-zeta potential recorder (Malvern, ZEN3690). A certain amount of the adsorbent was dispersed in distilled water with various pH values before this measurement. The elements of CMC and EDA-CMC$_1$ were analyzed by EDS (Quanta 200, FEI) equipped by SEM.

2.6. Adsorption isotherms

The Langmuir [17,21] and Freundlich isotherm [22,23] models have been widely used for analyzing adsorption data.

The Langmuir model assumes that there is no interaction between the adsorbate molecules and the adsorption is localized in a monolayer. The linear and nonlinear Langmuir equation could be expressed by Eqs. (3) and (4) as follows:

$$\frac{C_e}{q_e} = \frac{1}{q_m K_L} + \frac{C_e}{q_m}$$

(3)

$$q_e = \frac{K_L q_m C_e}{1 + C_e K_L} \qquad (4)$$

where q_e is the adsorption capacity in equilibrium state (mg g^{-1}), C_e represents the equilibrium concentration (mg L^{-1}), q_m is the maximal adsorbed amount of the adsorbent (mg g^{-1}), and K_L is the Langmuir adsorption constant. The separation factor represented by the dimensionless equilibrium parameter R_L is defined in Eq. (5).

$$R_L = \frac{1}{1 + K_L C_0} \qquad (5)$$

where C_0 represents the initial solute concentration. The adsorption process is unfavorable for $R_L > 1$, linear for $R_L = 1$, favorable for $0 < R_L < 1$, and irreversible when $R_L = 0$.

The Freundlich equation in linear and nonlinear is an empirical equation based on adsorption on a heterogeneous surface. The equation is commonly expressed in Eq. (6) as follows:

$$\log q_e = \log K_F + \frac{1}{n} \log C_e \qquad (6)$$

where q_e is the amount adsorbed at equilibrium (mg g^{-1}) and C_e is the equilibrium concentration of the adsorbate. K_F (mg g^{-1} (L mg^{-1})$^{1/n}$) is the adsorption capacity of the adsorbent. The n value is used to describe the nature of the adsorption process.

2.7. Adsorption kinetics

The modes of interactions between sorbent and sorbate are diverse and specific, thus various types of kinetic equations have been developed to describe the possible underlying mechanism of a given sorbent–sorbate system [24]. Here the kinetics data were analyzed by the pseudo-first-order (Eq. (7)) [25,26] and pseudo-second-order kinetic models (Eq. (8)) [23,27,28].

$$\ln(q_e - q_t) = \ln q_e - k_1 t \qquad (7)$$

$$\frac{t}{q_t} = \frac{1}{k_2 q_e^2} + \frac{t}{q_e} \qquad (8)$$

where q_e and q_t are the amounts of dye adsorbed on adsorbent (mg g^{-1}) at equilibrium and at time t, respectively, and k_1, k_2 are the rate constant of pseudo-first-order and pseudo-second-order kinetics, respectively.

3. Results and discussion

3.1. Optimization of adsorbent composition and dyes

The removal of ORII and MB on various CMC adsorbents was compared (Fig. 2(a)). The adsorption capacity of CMC before modification can hardly adsorb cationic or anionic dyes. After modification by EDA, the adsorption properties of CMC were significantly enhanced. With EDA/CMC ratio (mL g^{-1}) increased from 5/3 to 5/0.5, the removal of ORII increased from 27.83% to 66.26%, while MB removal varied from 88.28% to 83.99%. It may be due to that the amount of –COOH groups in EDA-CMC$_x$ decreased with EDA/CMC ratio increasing. This resulted in decrease of the adsorptive sites toward the cationic MB and then a decrease on the removal efficiency of MB [29,30]. The removal of ORII increased could be interpreted as: the electrostatic repulsions decreased between the adsorbent EDA-CMC$_x$ and the anionic dye ORII with EDA/CMC ratio increasing [31]. Moreover, –NH$_2$ group of EDA acted as the active sites in ORII adsorption [32]. These results indicated that both CMC and EDA were involved in the MB and ORII adsorption process. In addition, the amount of –COOH and –NH$_2$ groups in EDA-CMC$_x$ play an important role in the process of adsorption [16]. Considering the excellent adsorption property of EDA-CMC$_1$ toward both ORII and MB, the EDA-CMC$_1$ was selected in the further study.

At RT and original pHs, the adsorption of 10 mL 50 mg L^{-1} various dyes, including three anionic dyes (CR, MO, and ORII) and two cationic dyes (MG and MB), onto 30 mg EDA-CMC$_1$ within 60 min is shown in Fig. 2(b). It can be found that higher removal efficiencies of 62.05%, 82.69%, and 66.21% were obtained for MG, MB, and ORII, respectively. This result indicated that the electrostatic attraction was not the
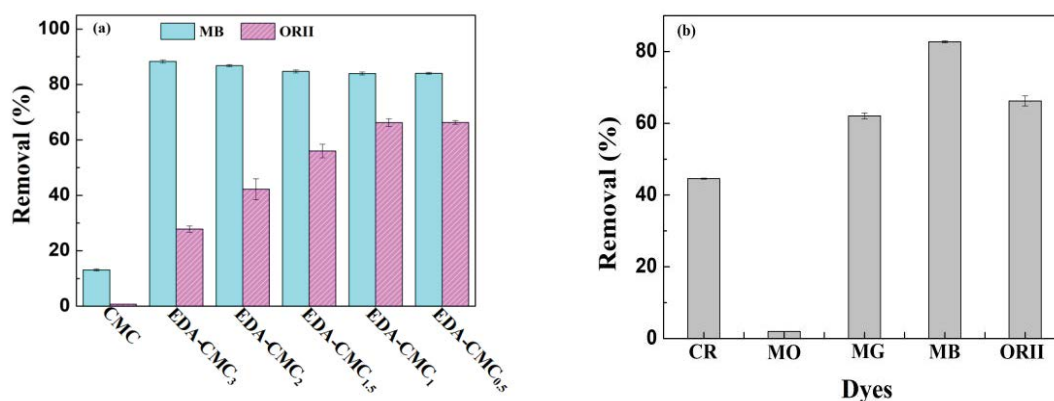

Fig. 2. Comparison of various CMC adsorbents toward ORII or MB (a) and various dyes adsorption onto EDA-CMC$_1$ (b) (30 mg adsorbent; 10 mL 50 mg L^{-1} dyes; room temperature; 60 min; original pH).

only interaction during the adsorption process. As an anionic dye, orange II is nonbiodegradable in nature and known to induce cytogenetic changes in animals, and extensively used in many fields. Being anionic in nature, orange II has high potential to leach into the soil profile and to contaminate ground water [33]. Methylene blue has been considered as a common cationic dye model in the adsorption studies owing to its planar form [16]. This structure makes MB readily aggregate and highly soluble in solutions even at micromolar concentrations, that causing harmful environmental effects. Therefore, MB and ORII were represented as cationic and anionic dye models to investigate the adsorption capacities of DEA-CMC$_1$ adsorbent.

3.2. Characterization of EDA-CMC$_1$

3.2.1. FT-IR spectra

The FT-IR spectra of CMC, EDA-CMC$_1$ before and after adsorption of ORII and MB are shown in Fig. 3. The broad band at 3,418 cm^{-1} was attributed to the stretching vibration of OH groups. Two bands at 2,936 and 2,986 cm^{-1} attributed to C–H stretching [34,35]. The band at 1,602 cm^{-1}, assigning to the stretching vibration of COO–, shifted to 1,604 and decreased obviously after EDA modification [36]. Moreover, a new band centered at 1,748 cm^{-1}, due to the C=O stretching vibration in amide groups, was appeared [19,37,38], indicating the successful modification of CMC by EDA. The stretching vibration of N–H was also located at 1,604 cm^{-1}. The absorption bands at 1,421, 1,325, and 1,057 cm^{-1} can be attributed to the asymmetric and symmetric stretching vibration of COO– and C–O–C group, respectively [39–41].

After ORII or MB adsorption, an absorption peak at 882 cm^{-1} attributed to C–H of benzene was detected [42]. Meanwhile, the –OH absorption peak at 3,418 cm^{-1} weakened, indicating the involvement of –OH during the adsorption process. The absorption peaks of N–H at 1,604 cm^{-1} and C=O group at 1,748 cm^{-1} were significantly weakened after the dye adsorption, which might be caused by the electrostatic attraction and hydrogen bond between the adsorbent
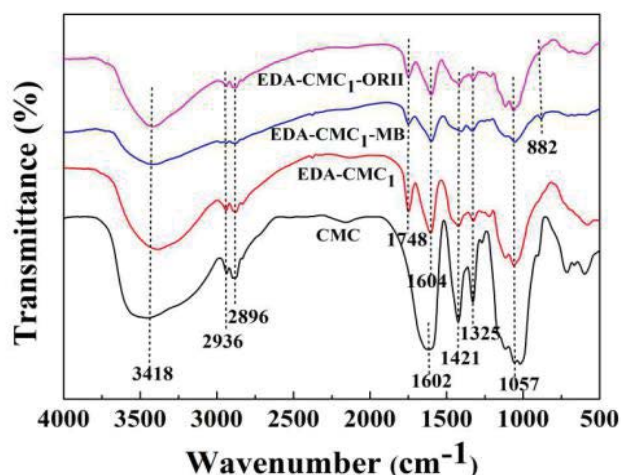
EDA-CMC$_1$ and the adsorbate. Thus, the amino, hydroxyl, and carboxyl groups in EDA-CMC$_1$ played an important role in the adsorption process [16].

3.2.2. SEM and EDS analysis

SEM images of CMC and EDA-CMC$_1$ are shown in Fig. 4. A rod-shaped structure and smooth surface morphology for CMC was observed (Figs. 4(a) and (b)) [43]. In contrast, the modified adsorbent EDA-CMC$_1$ exhibited a loose, massive concave–convex irregular bulk structure with rough surface, instead of the fibrous structure morphology for CMC (Figs. 4(c) and (d)) [19]. This indicated that EDA-CMC$_1$ had more active adsorption sites comparing with CMC, which increased the interaction between EDA-CMC$_1$ and dyes, thus improved dyes adsorption efficiency [44].

The elements content of CMC and EDA-CMC$_1$ analyzed quantitatively by energy dispersive spectroscopy (EDS) shown in Table 2 confirmed that 49.29 wt% carbon and 50.71 wt% oxygen in CMC, while decreased oxygen content (36.14 wt%) and appearing nitrogen component (14.66 wt%) for EDA-CMC$_1$, due to the replacement of –OH of –COOH by –NHCH$_2$CH$_2$NH$_2$ of EDA, were detected. This result indicated that amino group was successfully introduced into CMC [35].

3.2.3. TGA and zeta potential analysis

The TGA curves of CMC and EDA-CMC$_1$ are shown in Fig. 5. The first weight loss occurred between RT and 150°C, in which mass loss of 10.6 wt% and 7.1 wt% for CMC and EDA-CMC$_1$, respectively, corresponding to the loss of physically adsorbed water [38]. The second weight loss of 38.0 wt% for CMC was observed at 242°C–307°C, that was related to the release of water more firmly bound through the polar interactions with the carboxylate groups, in addition to the loss of CO$_2$ from the polysaccharides and decomposition of the cyclic products [45]. The second decomposition of EDA-CMC$_1$ occurred at 219°C–353°C, with a mass loss of 41.1 wt%, which was related to decomposition of the amino groups and the cellulose structure. The differences in weight losses and the range of temperature suggested that the modified chemicals have some effect on the pyrolysis behavior of CMC [14].

The zeta potential of EDA-CMC$_1$ versus pH values is shown in Fig. 5(b). With the increase of the pH value, the zeta potential decreased from +10 mV (pH3) to −30 mV (pH11) and the pH of zero point charge (pH$_{zpc}$) was 3.6. When pH < pH$_{zpc}$, EDA-CMC$_1$ exhibited positive charge, due to the protonation of amine (EDA-CMC$_1$-NH$_3^+$), that was beneficial to anionic dyes adsorption [46]. When pH > pH$_{zpc}$, negatively charged surface was conducive to the adsorption of cationic dyes, which was due to the deprotonation of carboxyl in EDA-CMC$_1$ [20].

3.3. Optimization of adsorption operation parameters

3.3.1. Effect of pH on the adsorption of ORII and MB

The initial pH of solution is an important parameter controlling the dye adsorption process, since it can affect the surface charge of the adsorbent, the ionization degree
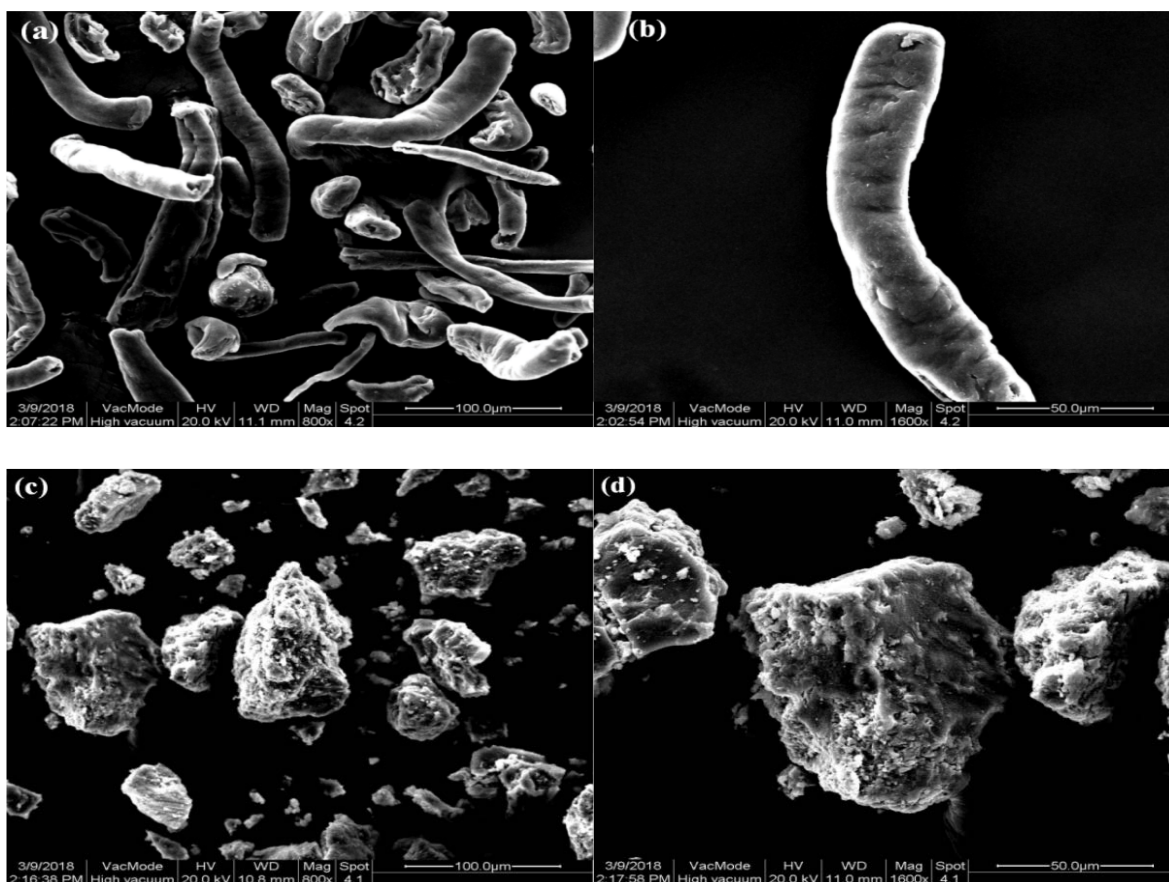

Fig. 3. FT-IR spectra of CMC, EDA-CMC$_1$ before and after adsorption.

Fig. 4. SEM images of CMC (a, b) and EDA-CMC$_1$ (c, d).

Table 2
Elemental analysis of CMC and EDA-CMC$_1$

Mass (%)	C	O	N
CMC	49.29	50.71	–
EDA-CMC$_1$	49.20	36.14	14.66

of different pollutants, the dissociation of functional groups on the active sites of the adsorbent, and the structure of the dye molecule. pH can not only greatly affect the removal efficiency of dyes, but also can affect the adsorption capacity of the adsorbent [47]. Therefore, the effect of solution pH (Figs. 6(a)–(c)) on removal of MB and ORII and adsorption capacity of EDA-CMC$_1$ adsorbent was investigated in the range of 3–11. It was found that the adsorption of MB
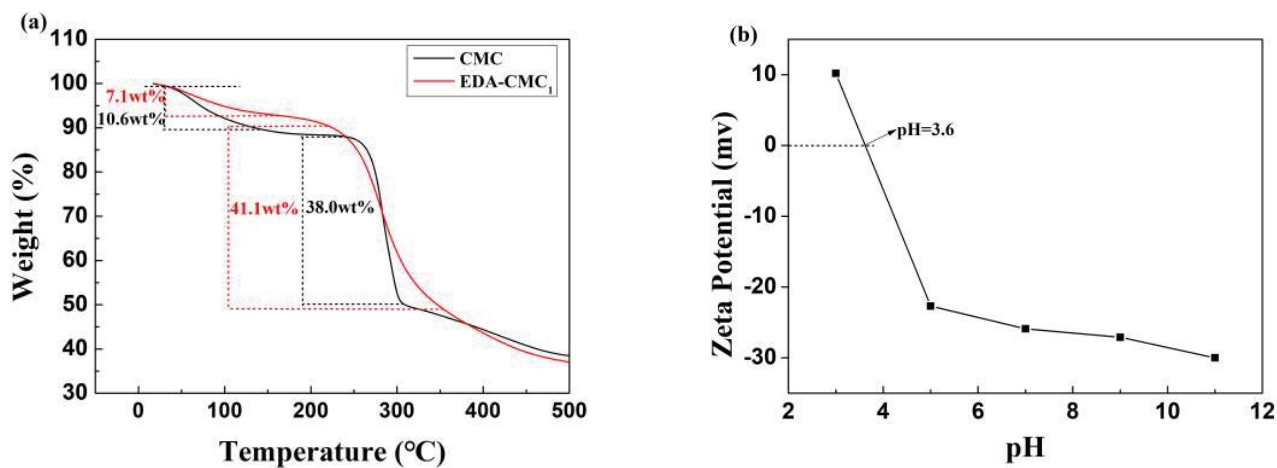

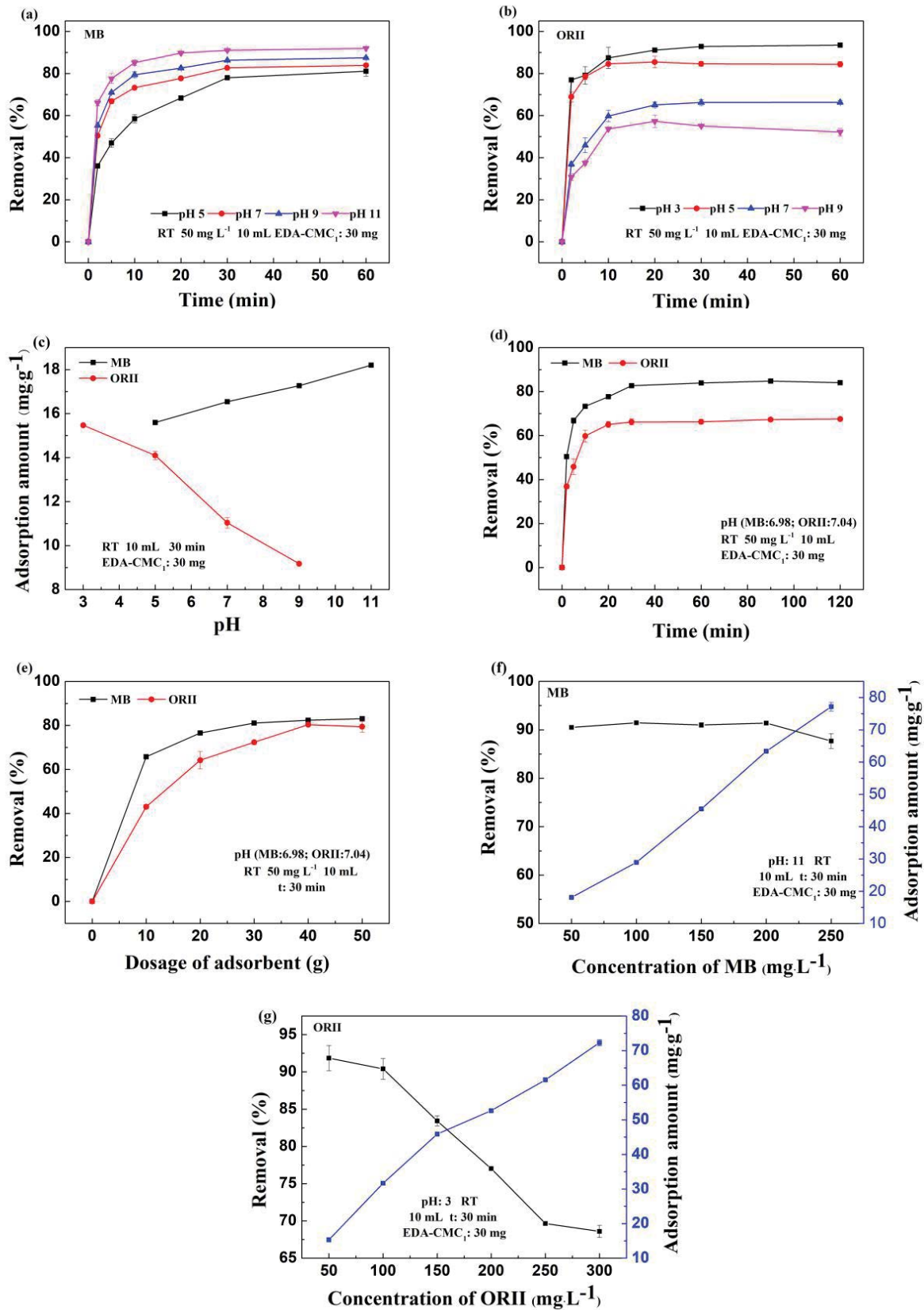Fig. 5. TGA curves (a) and zeta potential (b) of EDA-CMC$_1$ with various pHs.

Fig. 6. Effect of various parameters on MB and ORII adsorption onto EDA-CMC$_1$ (pH (a, b, and c), contact time (d), adsorbent dosage (e), initial dye concentration (f, g)).

on EDA-CMC$_1$ increased significantly with the increase of pH from 5 to 11, and the maximum removal of 91.94% and adsorption capacity of 18.20 mg g^{-1} were obtained at pH 11. On the contrary, the removal of ORII decreased with the increase of pH from 3 to 9, the maximum removal of 92.81% and adsorption capacity of 15.47 mg g^{-1} at pH 3 were observed, indicating that EDA-CMC$_1$ exhibited pH sensitivity. It was probably because at lower pH, the presence of H$^+$ ions will compete with cationic MB for adsorption sites. The EDA-CMC$_1$ surface was more negatively charged at higher pH, and improved the adsorption toward MB, since the electrostatic interaction between MB and adsorbent transferred from repulsion to attraction. For ORII, the adsorption amount decreased with pH increase. This might be due to that at high pH, OH$^-$ groups on the surface of the adsorbent will repel the anionic dye molecules [48]. These results were also confirmed by zeta potential analysis: at the lower pH conditions, the positively charged surface was in favor of anionic dye ORII adsorption, while negative charged surface at higher pH was beneficial to cationic dye MB adsorption.

At the same conditions, the removal of MB was higher than that of ORII (Figs. 6(a)–(c)), because zeta potential of EDA-CMC$_1$ was +10 mV at pH 3 and −30 mV at pH 11, respectively, as Fig. 5(b) shows. Positively charged surface was beneficial to remove anionic dyes, while negatively charged surface was in favor of adsorbing cationic dyes [49]. Moreover, higher charged surface exhibited stronger potential interaction. Therefore, the removal of MB was higher than that of ORII.

3.3.2. Effect of contact time on ORII and MB removal

Obviously, adsorption process was rapid at the initial 10 min, and then almost reached equilibrium within 30 min, 66.22% and 82.70% removal for ORII and MB, respectively, were obtained (Fig. 6(d)). In the first 10 min active adsorption sites are available for ORII and MB. With the contact time prolonging, adsorption sites are gradually occupied and inaccessible, thus adsorption rate kept constant [25,50]. Compared with most reported adsorbent [33,48], the adsorption rate of EDA-CMC$_1$ was moderate and feasible in the real application. Therefore, the optimal contact time was 30 min.

3.3.3. Effect of the adsorbent dosage on ORII and MB removal

The effect of adsorbent EDA-CMC$_1$ dosages on ORII and MB removal (Fig. 6(e)) indicated that the dye removal increased with dosage increasing. This might be due to that the number of adsorption sites increased with the increase of the dosage of adsorbent [50]. But further increase the adsorbent dose, the dye removal was almost unchanged, so those dosages (40 mg for ORII; 30 mg for MB) were considered as the optimum dose [51].

3.3.4. Effect of initial concentration of dye on adsorption capacity and dye removal

The effect of initial concentration of dye on adsorption capacity and removal (Figs. 6(f) and (g)) showed that the

adsorption capacity increased with initial concentration of ORII and MB increasing. The uptake of ORII and MB increased from 15.31 to 72.26 mg g^{-1} and 18.10 to 77.18 mg g^{-1}, respectively, with the initial concentration increased from 50 to 300 (ORII) or 250 mg L^{-1} (MB) at 30 min. The removal of MB decreased slightly from 90.50% to 87.70% with MB increasing from 50 to 250 mg L^{-1}, while the removal of ORII decreased obviously from 91.86% to 68.60% with ORII increasing from 50 to 300 mg L^{-1} at 30 min. That means the adsorption process is highly dependent on the initial concentration that may be attributed to the high mass transfer driving force [27]. In fact, at a certain adsorbent dosage, the adsorption sites were sufficient for adsorption of ORII and MB molecules at lower initial concentration, and the uptake of ORII and MB molecules depended on the amount of ORII and MB transferring from solution to the surface of adsorbent [52]. The removal of ORII and MB decreased due to the active sites of adsorbent were less available [53], hence more dye molecules left unadsorbed in the solution, and dyes removal decreased.

3.4. Adsorption isotherms

The adsorption isotherms in linear and nonlinear fitting patterns, and calculated parameters coefficients are given in Fig. 7 and Table 3, respectively. The coefficient of linear Langmuir model (R^2) was closer to 1 than other models for ORII adsorption, and the calculated q_m from nonlinear Langmuir model was close to the experimental data $q_{e,\exp}$. The separation factor R_L of linear and nonlinear fitting isotherms was in the range of 0–1, indicated that the adsorption process was favorable [54]. The factor $n > 1$ of Freundlich implied that the adsorption of ORII was favorable and could also be described by Freundlich isotherm model. This phenomenon indicated that ORII adsorption process was complicated. For MB adsorption, the coefficient (R^2) of nonlinear Langmuir model was closer to 1 than those of others, but large differences were observed between calculated q_m and experimental data $q_{e,\exp}$. The R^2 derived from linear and nonlinear Freundlich model both were higher than 0.9, moreover, $n > 1$, indicated adsorption process was favorable. So the Freundlich model fitted better than Langmuir isotherm [55], indicating that the adsorbent surface was heterogeneous [56].

3.5. Adsorption kinetics

The kinetics plots and the parameters are given in Fig. 8 and Table 4, respectively. The results indicated that the adsorption process of MB and ORII onto EDA-CMC$_1$ exhibited excellent compliance with pseudo-second-order kinetics equation with regression coefficients (R^2) higher than 0.99, indicating the adsorption involved chemical reaction between functional groups presented on the adsorbent surface and the dyes molecules [27].

3.6. Comparison with various adsorbents

The comparison of the adsorption efficiency of EDA-CMC$_1$ toward MB and ORII with some of the reported adsorbents is summarized in Table 5. It was observed that
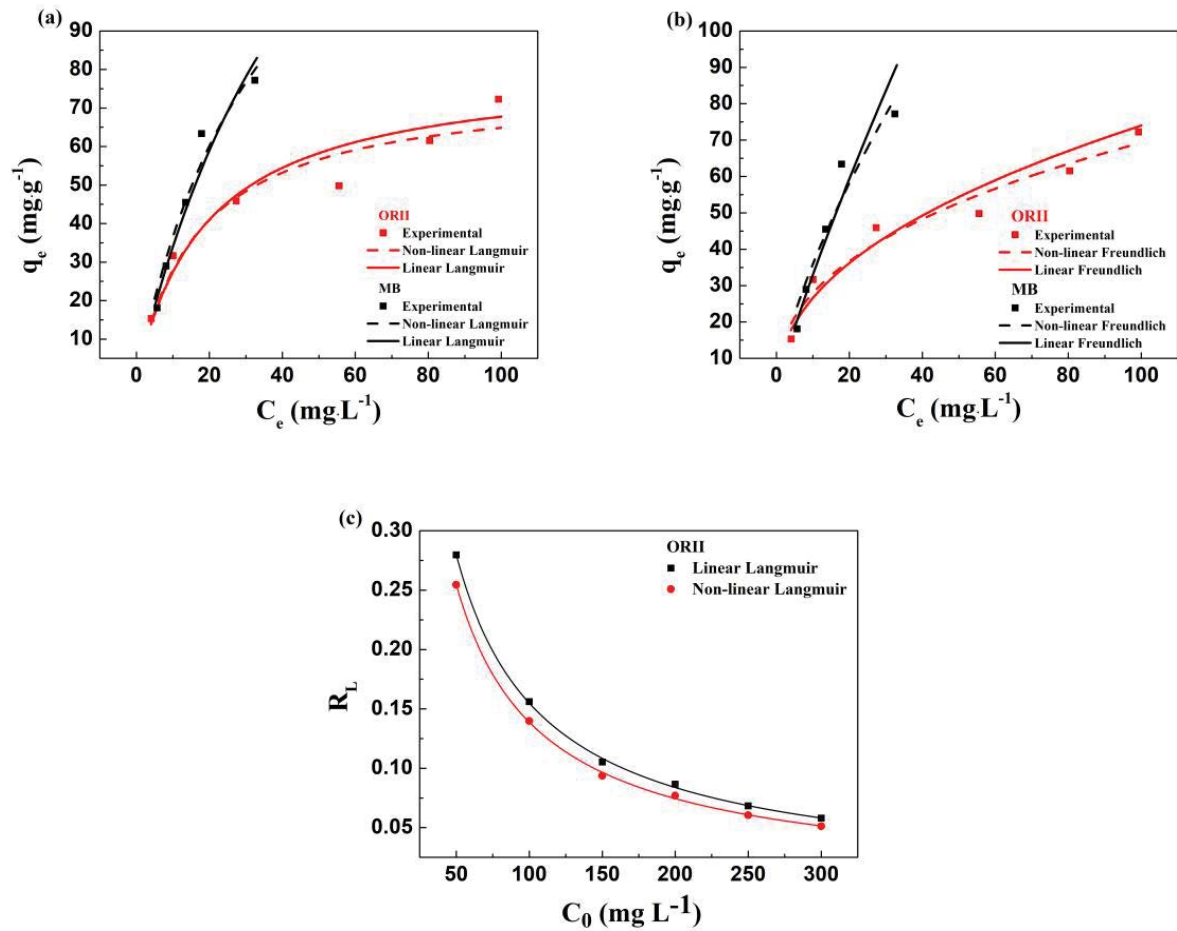
Fig. 7. Langmuir (a) and Freundlich (b) isotherms for dyes adsorption onto EDA-CMC$_1$; the separation factor R_L of linear and nonlinear Langmuir isotherms for ORII (c) (10 mL; 30 min; room temperature; pH (ORII 3 and MB 11)).

Table 3
Langmuir and Freundlich isotherms parameters for dyes removal by EDA-CMC$_1$

		Langmuir		Freundlich		Experiment
		Linear	Nonlinear	Linear	Nonlinear	$q_{e,\exp}$
ORII	Isotherms parameters R^2	q_m = 80.91 mg g^{-1} K_L = 0.0515 L mg^{-1} 0.9758	q_m = 75.95 mg g^{-1} K_L = 0.0586 L mg^{-1} 0.9171	n = 2.2503 K_F = 9.5799 0.9489	n = 2.5379 K_F = 11.2900 0.9455	72.26
MB	Isotherms parameters R^2	q_m = 223.24 mg g^{-1} K_L = 0.0180 L mg^{-1} 0.5422	q_m = 169.71 mg g^{-1} K_L = 0.0275 L mg^{-1} 0.9480	n = 1.1810 K_F = 4.6954 0.9335	n = 1.4376 K_F = 7.2384 0.9124	77.18

excellent adsorption capacity of EDA-CMC$_1$ exhibited than those of reported works. The adsorbent in this study presented amphoteric adsorption properties and could adsorb anionic dyes and cationic dyes simultaneously. Moreover, the adsorption equilibrium could be reached within 30 min, faster than most of the reported adsorbents, indicating that the ethylenediamine-modified CMC in our study could be used as a potential adsorbent in the real dyeing wastewater treatment.

3.7. Regeneration studies

Recyclable adsorbents were highly desired in the industry for the removal of dyes. Fig. 9 describes the results of the EDA-CMC$_1$ regeneration study, more than 90% MB removal and 70% ORII removal could be achieved after 5 adsorption–desorption cycles. Sorption–desorption test indicated that the dye molecules absorbed on the surface of EDA-CMC$_1$ could be successfully desorbed and the EDA-CMC$_1$ could
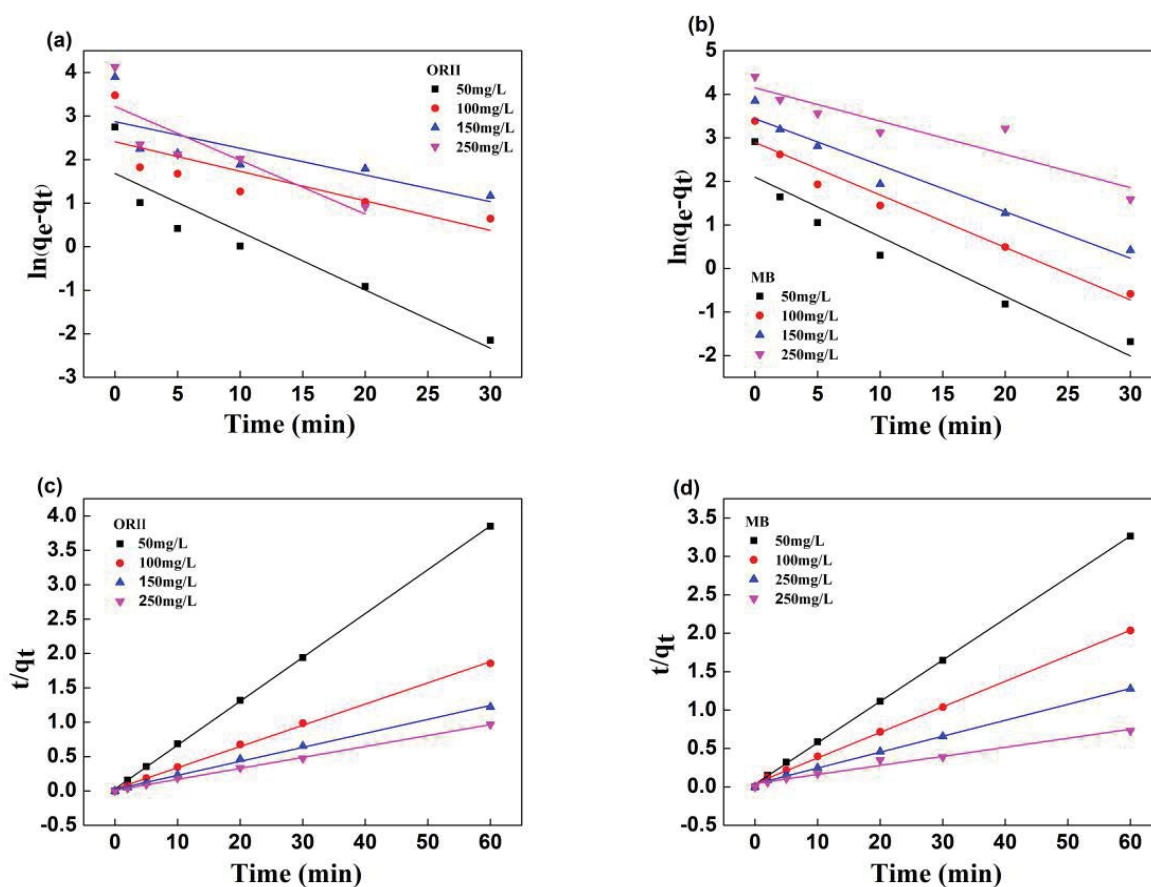
Fig. 8. The pseudo-first-order (a, b) and pseudo-second-order model (c, d) for adsorption of ORII and MB onto EDA-CMC$_1$ (10 mL; room temperature; pH (ORII 3 and MB 11)).

Table 4
Kinetic parameters for the removal of ORII and MB by EDA-CMC$_1$

	C_0 (mg L^{-1})	Pseudo-first-order model			Experiment	Pseudo-second-order model		
		$q_{e,1}$	k_1	R^2	$q_{e,\exp}$	$q_{e,2}$	k_2	R^2
ORII	50	5.38	0.1338	0.8392	15.59	15.68	34.471	0.9998
	100	8.16	0.0678	0.5464	32.35	32.41	33.829	0.9983
	150	17.69	0.0613	0.5103	49.08	49.16	42.088	0.9970
	250	25.03	0.1235	0.6348	63.72	62.77	101.626	0.9988
MB	50	8.16	0.1370	0.8972	18.39	18.57	28.323	0.9997
	100	18.05	0.1205	0.9458	29.49	30.06	22.553	0.9989
	150	31.19	0.1068	0.9384	47.02	48.26	26.302	0.9978
	250	63.34	0.0764	0.8318	82.06	84.81	22.847	0.9767

be regenerated facilely, which further confirmed its potential applications in real wastewater treatment.

3.8. Possible adsorption mechanism

Based on the above discussions, a possible adsorption mechanism was proposed (Fig. 10). After modified CMC by EDA, the cationic MB molecules could be adsorbed onto the surface by electrostatic attractions with carboxylate groups,

which dominate the whole adsorption process [58]. And the number of positive charges at the adsorbent surface enhanced with EDA introducing, thus electrostatic attraction between adsorbent and anionic ORII dye molecule increased, due to the presence of sulfonate anions in dye structure and protonated groups as amine in adsorbent structure [61]. The hydroxyl groups in EDA-CMC$_1$ also participated in the interaction with N or O atom in dyes in hydrogen bonding form that was confirmed by FT-IR spectra, as Fig. 10 shows.

Table 5
Comparison of various adsorbents toward ORII and MB

| Adsorbents	Dyes	Adsorption conditions	Equilibration time	q_{max} (mg g^{-1})	References
CMC coated Fe$_3$O$_4$@SiO$_2$ MNPs	MB	pH 9–11; 350 K	60 min	22.7	[57]
Porous CMC-based hydrogels beads	MB	pH 7	24 h	82.3	[58]
magnetic nanocomposite hydrogels	MB	pH 7; 298 K	60 min	251.0	[59]
SDBS-zeolite	MB	pH 6.85; 298 K	60 min	15.7	[48]
EDA-CMC$_1$	MB	pH 11; 293 K	30 min	82.1	This study
EDA-CMC$_1$	ORII	pH 3; 293 K	30 min	63.7	This study
ODTMA-palygorskite (200% CEC)	ORII	pH 6.13; 298 K	5 h	99.0	[33]
HCZ	ORII	pH 1; 303 K	60 min	38.96	[60]
HDTMA-zeolite	ORII	pH 1; 308 K	1 h	3.38	[48]
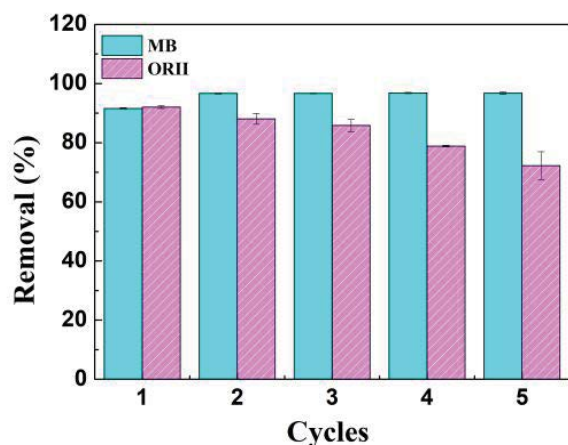
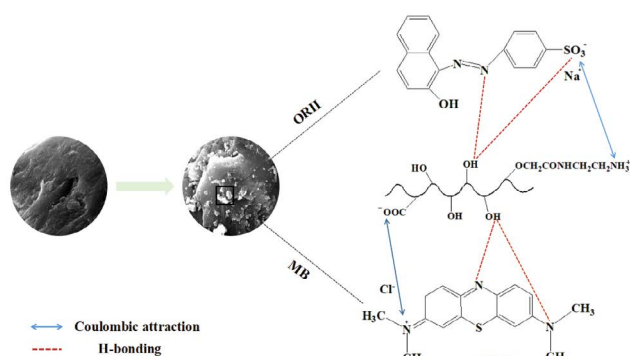Fig. 9. Sorption–desorption cycles of EDA-CMC$_1$.

Fig. 10. Possible interactions of ORII and MB with EDA-CMC$_1$.

4. Conclusion

The CMC was chemically modified to facilitate the removal of ORII and MB from aqueous solution. The prepared composites were characterized by various techniques such as FTIR, TGA, SEM, EDS, and zeta potential to investigate their structures and morphologies. EDA-CMC$_1$ presented amphoteric adsorption properties and exhibited strong affinity for ORII and MB molecules with pH sensitivity. At 293 K, the maximum adsorption capacities of 82.06 and 63.72 mg g^{-1} for MB and ORII, respectively, were obtained within 30 min, more than 90% MB and 70% ORII were removed after five cycles. Kinetic study showed that the pseudo-second-order kinetic model described better the adsorption process of ORII and MB. Adsorbent EDA-CMC$_1$ could be used as a potential adsorbent in the dyeing wastewater treatment with excellent adsorption performance.

References

[1] S.M. Twang, M.A.A. Zaini, L.M. Salleh, M.A.C. Yunus, M. Naushad, Potassium hydroxide-treated palm kernel shell sorbents for the efficient removal of methyl violet dye, Desal. Wat. Treat., 84 (2017) 262–270.

[2] A. Sharma, G. Sharma, M. Naushad, A.A. Ghfar, D. Pathania, Remediation of anionic dye from aqueous system using bio-adsorbent prepared by microwave activation, Environ. Technol., 39 (2018) 917–930.

[3] A.B. Albadarin, M. Charara, B.M.A. Tarboush, M.N.M. Ahmad, T.A. Kurniawan, N. Mu, G.M. Walker, C. Mangwandi, Mechanism analysis of tartrazine biosorption onto masau stones; a low cost by-product from semi-arid regions, J. Mol. Liq., 242 (2017) 478–483.

[4] L. Wang, J. Li, Adsorption of CI Reactive Red 228 dye from aqueous solution by modified; cellulose from flax shive: kinetics, equilibrium, and thermodynamics, Ind. Crop Prod., 42 (2013) 153–158.

[5] A. Salama, N. Shukry, M. Elsakhawy, Carboxymethyl cellulose-g-poly(2-(dimethylamino) ethyl methacrylate) hydrogel as adsorbent for dye removal, Int. J. Biol. Macromol., 73 (2015) 72–75.

[6] M. Naushad, Z.A. Alothman, M.R. Awual, S.M. Alfadul, T. Ahamad, Adsorption of rose Bengal dye from aqueous solution by amberlite Ira-938 resin: kinetics, isotherms, and thermodynamic studies, Desal. Wat. Treat., 57 (2016) 13527–13533.

[7] A.A. Alqadami, N. Mu, M.A. Abdalla, M.R. Khan, Z.A. Alothman, Adsorptive removal of toxic dye using Fe$_3$O$_4$–TSC nanocomposite: equilibrium, kinetic, and thermodynamic studies, J. Chem. Eng. Data, 61 (2016) 3806–3813.

[8] E. Daneshvar, A. Vazirzadeh, A. Niazi, M. Kousha, N. Mu, A. Bhatnagar, Desorption of Methylene blue dye from brown macroalga: effects of operating parameters, isotherm study and kinetic modeling, J. Cleaner Prod., 152 (2017) 443–453.

[9] T.M. Missimer, R.G. Maliva, A.H.A. Dehwah, D. Phelps, Use of beach galleries as an intake for future seawater desalination facilities in Florida and globally similar areas, Desal. Wat. Treat., 52 (2014) 1–8.

[10] D. Pathania, G. Sharma, A. Kumar, M. Naushad, S. Kalia, A. Sharma, Z.A. Alothman, Combined sorptional-photocatalytic remediation of dyes by polyaniline Zr(IV)

selenotungstophosphate nanocomposite, Toxicol. Environ. Chem. Rev., 97 (2015) 526–537.

[11] H. Javadian, M.T. Angaji, M. Naushad, Synthesis and characterization of polyaniline/γ-alumina nanocomposite: a comparative study for the adsorption of three different anionic dyes, J. Ind. Eng. Chem., 20 (2014) 3890–3900.

[12] A. Bhatnagar, E. Kumar, M. Sillanpää, Fluoride removal from water by adsorption – a review, Chem. Eng. J., 171 (2011) 811–840.

[13] A.B. Albadarin, M.N. Collins, N. Mu, S. Shirazian, G. Walker, C. Mangwandi, Activated lignin–chitosan extruded blends for efficient adsorption of methylene blue, Chem. Eng. J., 307 (2016) 264–272.

[14] Q.Q. Zhong, Q.Y. Yue, Q. Li, B.Y. Gao, X. Xu, Removal of Cu(II) and Cr(VI) from wastewater by an amphoteric sorbent based on cellulose-rich biomass, Carbohydr. Polym., 111 (2014) 788–796.

[15] H.S. Lee, J.I. Choi, J.H. Kim, K.W. Lee, Y.J. Chung, M.H. Shin, M.W. Byun, M.G. Shin, J.W. Lee, Investigation on radiation degradation of carboxymethylcellulose by ionizing irradiation, Appl. Radiat. Isot., 67 (2009) 1513–1515.

[16] C. Liu, A.M. Omer, X.K. Ouyang, Adsorptive removal of cationic methylene blue dye using carboxymethyl cellulose/k-carrageenan/activated montmorillonite composite beads: isotherm and kinetic studies, Int. J. Biol. Macromol., 106 (2017) 823–833.

[17] W. Li, P. Zuo, D. Xu, Y. Xu, K. Wang, Y. Bai, H. Ma, Tunable adsorption properties of bentonite/carboxymethyl cellulose-g-poly(2-(dimethylamino) ethyl methacrylate) composites towards anionic dyes, Chem. Eng. Res. Des., 124 (2017) 260–270.

[18] J.L. Yan, G.J. Chen, J. Cao, W. Yang, B.H. Xie, M.B. Yang, Functionalized graphene oxide with ethylenediamine and 1,6-hexanediamine, New Carbon Mater., 52 (2012) 624.

[19] T. Velempini, K. Pillay, X.Y. Mbianda, O.A. Arotiba, Epichlorohydrin crosslinked carboxymethyl cellulose-ethylene-diamine imprinted polymer for the selective uptake of Cr(VI), Int. J. Biol. Macromol., 101 (2017) 837–844.

[20] W. Wei, S. Kim, M.H. Song, J.K. Bediako, Y.S. Yun, Carboxymethyl cellulose fiber as a fast binding and biodegradable adsorbent of heavy metals, J. Taiwan Inst. Chem. Eng., 57 (2015) 104–110.

[21] C. Namasivayam, D. Kavitha, Removal of Congo Red from water by adsorption onto activated carbon prepared from coir pith, an agricultural solid waste, Dyes Pigm., 54 (2002) 47–58.

[22] T. Liu, Y. Li, Q. Du, J. Sun, Y. Jiao, G. Yang, Z. Wang, Y. Xia, W. Zhang, K. Wang, Adsorption of methylene blue from aqueous solution by graphene, Colloids Surf., B, 90 (2012) 197–203.

[23] A.P. Vieira, S.A. Santana, C.W. Bezerra, H.A. Silva, J.A. Chaves, J.C. de Melo, S.F.E. Da, C. Airoldi, Kinetics and thermodynamics of textile dye adsorption from aqueous solutions using babassu coconut mesocarp, J. Hazard. Mater., 166 (2009) 1272–1278.

[24] N.A. Oladoja, A critical review of the applicability of Avrami fractional kinetic equation in adsorption-based water treatment studies, Desal. Wat. Treat., 57 (2015) 1–13.

[25] Y. Wang, Y. Feng, X.F. Zhang, X. Zhang, J. Jiang, J. Yao, Alginate-based attapulgite foams as efficient and recyclable adsorbents for the removal of heavy metals, J. Colloid Interface Sci., 514 (2018) 190–198.

[26] Z.J. Shao, X.L. Huang, F. Yang, W.F. Zhao, X.Z. Zhou, C.S. Zhao, Engineering sodium alginate-based cross-linked beads with high removal ability of toxic metal ions and cationic dyes, Carbohydr. Polym., 187 (2018) 85–93.

[27] Y.H. Magdy, H. Altaher, Kinetic analysis of the adsorption of dyes form high strength wastewater on cement kiln dust, J. Environ. Chem. Eng., 6 (2018) 834–841.

[28] Y.S. Ho, G. Mckay, Pseudo-second order model for sorption processes, Process Biochem., 34 (1999) 451–465.

[29] N. Gong, Y. Liu, R. Huang, Simultaneous adsorption of Cu²⁺ and Acid fuchsin (AF) from aqueous solutions by CMC/bentonite composite, Int. J. Biol. Macromol., 115 (2018) 580–589.

[30] Y. Liu, W.B. Wang, A.Q. Wang, Adsorption of lead ions from aqueous solution by using carboxymethyl cellulose-g-poly (acrylic acid)/attapulgite hydrogel composites, Desalination, 259 (2010) 258–264.

[31] K. Varaprasad, T. Jayaramudu, E.R. Sadiku, Removal of dye by carboxymethyl cellulose, acrylamide and graphene oxide via a free radical polymerization process, Carbohydr. Polym., 164 (2017) 186–194.

[32] K. Liu, L. Chen, L. Huang, Y. Lai, Evaluation of ethylenediamine-modified nanofibrillated cellulose/chitosan composites on adsorption of cationic and anionic dyes from aqueous solution, Carbohydr. Polym., 151 (2016) 1115–1119.

[33] B. Sarkar, Y. Xi, M. Megharaj, R. Naidu, Orange II adsorption on palygorskites modified with alkyl trimethylammonium and dialkyl dimethylammonium bromide – an isothermal and kinetic study, Appl. Clay Sci., 51 (2011) 370–374.

[34] I.A. Udoetok, R.M. Dimmick, L.D. Wilson, J.V. Headley, Adsorption properties of cross-linked cellulose-epichlorohydrin polymers in aqueous solution, Carbohydr. Polym., 136 (2016) 329–340.

[35] Z. Ding, R. Yu, X. Hu, Y. Chen, Y. Zhang, Graft copolymerization of epichlorohydrin and ethylenediamine onto cellulose derived from agricultural by-products for adsorption of Pb(II) in aqueous solution, Cellulose, 21 (2014) 1459–1469.

[36] A.M.A. Ghaffar, M.B. Elarnaouty, A.A.A. Baky, S.A. Shama, Radiation-induced grafting of acrylamide and methacrylic acid individually onto carboxymethyl cellulose for removal of hazardous water pollutants, Des. Monomers Polym., 19 (2016) 1–13.

[37] N. Li, G. Chen, W. Chen, J. Huang, J. Tian, X. Wan, M. He, H. Zhang, Multivalent cations-triggered rapid shape memory sodium carboxymethyl cellulose/polyacrylamide hydrogels with tunable mechanical strength, Carbohydr. Polym., 178 (2017) 159–165.

[38] A. Casaburi, Ú. Montoya Rojo, P. Cerrutti, A. Vázquez, M.L. Foresti, Carboxymethyl cellulose with tailored degree of substitution obtained from bacterial cellulose, Food Hydro-colloid, 75 (2018) 147–156.

[39] S. Yang, S. Fu, Y. Zhou, C. Xie, X. Li, Preparation and release properties of a pH-tunable carboxymethyl cellulose hydrogel/methylene blue host/guest model, Int. J. Polym. Mater. Pol., 60 (2010) 62–74.

[40] Q. Lin, M. Gao, J. Chang, H. Ma, Adsorption properties of crosslinking carboxymethyl cellulose grafting dimethyldially-lammonium chloride for cationic and anionic dyes, Carbohydr. Polym., 151 (2016) 283–294.

[41] S. Mishra, G.U. Rani, G. Sen, Microwave initiated synthesis and application of polyacrylic acid grafted carboxymethyl cellulose, Carbohydr. Polym., 87 (2012) 2255–2262.

[42] R. Suresh, K. Giribabu, R. Manigandan, S.P. Kumar, S. Munusamy, S. Muthamizh, V. Narayanan, Polyaniline nanorods: synthesis, characterization, and application for the determination of para-nitrophenol, Anal. Lett., 49 (2016) 269–281.

[43] B. Wang, X. Yang, C. Qiao, Y. Li, T. Li, C. Xu, Effects of chitosan quaternary ammonium salt on the physicochemical properties of sodium carboxymethyl cellulose-based films, Carbohydr. Polym., 184 (2018) 37–46.

[44] J. Wang, X. Lin, X. Luo, Y. Long, A sorbent of carboxymethyl cellulose loaded with zirconium for the removal of fluoride from aqueous solution, Chem. Eng. J., 252 (2014) 415–422.

[45] S. Benghanem, A. Chetouani, M. Elkolli, M. Bounekhel, D. Benachour, Grafting of oxidized carboxymethyl cellulose with hydrogen peroxide in presence of Cu(II) to chitosan and biological elucidation, Biocybern. Biomed. Eng., 37 (2017) 94–102.

[46] L. Jin, W. Li, Q. Xu, Q. Sun, Amino-functionalized nanocrystalline cellulose as an adsorbent for anionic dyes, Cellulose, 22 (2015) 2443–2456.

[47] Y. Zong, Y. Zhang, X. Lin, D. Ye, X. Luo, J. Wang, Preparation of a novel microsphere adsorbent of prussian blue capsulated in carboxymethyl cellulose sodium for Cs(I) removal from contaminated water, J. Radioanal. Nucl. Chem., 311 (2016) 1–15.

[48] X. Jin, M.Q. Jiang, X.Q. Shan, Z.G. Pei, Z. Chen, Adsorption of methylene blue and orange II onto unmodified and surfactant-modified zeolite, J. Colloid Interface Sci., 328 (2008) 243–247.

[49] A. Salama, Preparation of CMC-g-P (SPMA) super adsorbent hydrogels: exploring their capacity for MB removal from waste water, Int. J. Biol. Macromol., 106 (2018) 940–946.

[50] M.E. El-Naggar, E.K. Radwan, S.T. El-Wakeel, H. Kafafy, T.A. Gad-Allah, A.S. El-Kalliny, T.I. Shaheen, Synthesis, characterization and adsorption properties of microcrystalline cellulose based nanogel for dyes and heavy metals removal, Int. J. Biol. Macromol., 113 (2018) 1–22.

[51] M. Zubair, N. Jarrah, Ihsanullah, A. Khalid, M.S. Manzar, T.S. Kazeem, M.A. Harthi, Starch–NiFe-layered double hydroxide composites: efficient removal of methyl orange from aqueous phase, J. Mol. Liq., 249 (2018) 254–264.

[52] X. Wan, Y. Zhan, Z. Long, G. Zeng, Y. He, Core@double-shell structured magnetic halloysite nanotube nano-hybrid as efficient recyclable adsorbent for methylene blue removal, Chem. Eng. J., 330 (2017) 491–504.

[53] K. Vijayalakshmi, B.M. Devi, S. Latha, T. Gomathi, P.N. Sudha, J. Venkatesan, S. Anil, Batch adsorption and desorption studies on the removal of lead (II) from aqueous solution using nanochitosan/sodium alginate/microcrystalline cellulose beads, Int. J. Biol. Macromol., 104 (2017) 1483–1494.

[54] S.A. Ali, I. Rachman, T. Saleh, Simultaneous trapping of Cr(III) and organic dyes by a pH-responsive resin containing zwitterionic aminomethylphosphonate ligands and hydrophobic pendants, Chem. Eng. J., 330 (2017) 663–674.

[55] S. Hokkanen, A. Bhatnagar, A. Koistinen, T. Kangas, U. Lassi, M. Sillanpää, Comparison of adsorption equilibrium models and error functions for the study of sulfate removal by calcium hydroxyapatite microfibrillated cellulose composite, Environ. Technol., 39 (2018) 952–966.

[56] G. Annadurai, R.S. Juang, D.J. Lee, Use of cellulose-based wastes for adsorption of dyes from aqueous solutions, J. Hazard. Mater., 92 (2002) 263–274.

[57] M. Zirak, A. Abdollahiyan, B. Eftekhari-Sis, M. Saraei, Carboxymethyl cellulose coated Fe_3O_4@SiO_2 core–shell magnetic nanoparticles for methylene blue removal: equilibrium, kinetic, and thermodynamic studies, Cellulose, 25 (2018) 503–515.

[58] T. Benhalima, H. Ferfera-Harrar, D. Lerari, Optimization of carboxymethyl cellulose hydrogels beads generated by an anionic surfactant micelle templating for cationic dye uptake: swelling, sorption and reusability studies, Int. J. Biol. Macromol., 23 (2017) 2558–2564.

[59] G.R. Mahdavinia, M. Soleymani, M. Sabzi, H. Azimi, Z. Atlasi, Novel magnetic polyvinyl alcohol/laponite RD nanocomposite hydrogels for efficient removal of methylene blue, J. Environ. Chem. Eng., 5 (2017) 2617–2630.

[60] X. Jin, B. Yu, Z. Chen, J.M. Arocena, R.W. Thring, Adsorption of Orange II dye in aqueous solution onto surfactant-coated zeolite: characterization, kinetic and thermodynamic studies, J. Colloid Interface Sci., 435 (2014) 15–20.

[61] A.A. Mir, A.A. Amooey, S. Ghasemi, Adsorption of direct yellow 12 from aqueous solutions by an iron oxide-gelatin nanoadsorbent; kinetic, isotherm and mechanism analysis, J. Cleaner Prod., 170 (2018) 570–580.